Noise Resistant Identification of Human Iris Patterns Using Fuzzy ARTMAP Neural Network

Arash Taherian and Mahdi Aliyari Sh.

Department of Electrical and Computer Engineering, Islamic Azad University, South Tehran Branch, Tehran, Iran
taherian_arash@yahoo.com, aliyari@eetd.kntu.ac.ir

Abstract

A biometric system provides automatic identification of an individual based on unique features or characteristics possessed by that person. Iris recognition is regarded as one of the most reliable and accurate biometric systems available. This paper, proposes an efficient iris recognition system that employs circular Hough transform technique to localize the iris region in the eye image and cumulative sum based gray change analysis method to extract features from the normalized iris template and also fuzzy ARTMAP neural network to classify the iris codes. The results of simulations on a set of 756 eye images illustrate that an accurate and noise resistant personal identification system has been successfully designed. The proposed system achieved 0 false acceptance rate using 1800-bit binary iris codes and recognized all authorized users with 100% accuracy.

Keywords: *Biometrics, Cumulative sum based gray change analysis, Fuzzy ARTMAP neural network, Incremental learning, Iris recognition, Noise resistance*

1. Introduction

Biometrics technology plays an important role in public security and information security domains. Using various physiological characteristics of human, such as speech, fingerprint, hand geometry, face, iris, retina, etc., biometrics accurately identifies each individual and distinguishes one from another [1].

Iris recognition is one of the important biometric approaches in human identification and has become very active topic in research and practical application. Iris region is the area between the pupil and the sclera and because it is made of many minute characteristics, this field is sometimes called iris texture [2]. These visible characteristics are not only unique for each subject but also unique for each eye of a subject and remain almost stable from six months of age to death. Such unique feature in the anatomical structure of the iris facilitates the differentiation among individuals [3].

Compared with other biometric features, iris patterns are more stable and reliable and unrelated to health or the environment. Iris recognition systems are noninvasive to their users, but do require a cooperative subject. Because of such unique features, iris recognition has become one of the most reliable and acceptable biometric approaches among users [4].

Iris recognition system consists of image acquisition, localization of the iris region in a digital eye image, feature extraction from normalized and enhanced iris template and classification of iris codes [5].

A variety of techniques have been developed for iris localization. In [3, 6-10], the system with circular edge detector, in [11] a gradient based Hough transform are used for the localizing of the iris. Also circular Hough transform [12, 13], random Hough transform are applied to find the iris circles and complete the iris localization. In [11, 14] Canny operator is used to locate the pupil boundary.

For feature extraction and pattern matching processes, various algorithms have been also applied. These methods use local and global features of the iris. Using phase based approach [3, 6-10], wavelet transform zero crossing approach [15,16], Gabor filtering [14], texture analysis based methods [12, 14-19] the solving of the iris recognition problem is considered. In [20, 21, 22] independent component analysis is proposed for iris recognition. Daugman [3, 6-10] used multiscale quadrature wavelets to extract texture phase structure information of the iris to generate a 2,048-bit iris code and compared the difference between a pair of iris representations by computing their Hamming distance. Boles and Boashash [15] calculated a zero-crossing representation of 1D wavelet transform at various resolution levels of a concentric circle on an iris image to characterize the texture of the iris. Iris matching was based on two dissimilarity functions. Sanchez-Avila and Sanchez-Reillo [16] further developed the method of Boles and Boashash by using different distance measures, such as Euclidean distance and Hamming distance, for matching. Wildes, *et al.*, [12] represented the iris texture with a Laplacian pyramid constructed with four different resolution levels and used the normalized correlation to determine whether the input image and the model image are from the same class. In this paper a combination of accurate and noise resistant methods is used for feature extraction and classification of iris codes.

2. Iris Recognition Process

Identification process begins with the eye image acquisition; this stage includes the near-infrared (NIR) lighting system, the positioning system and the physical capture system. Images are captured and saved in grayscale format and then are presented to the system. In this case an 8-bit code presents the brightness of each pixel; consequently, the resulting image will be composed of the gray shades. Pre-processing of the captured image is the next step; this stage includes iris localization, normalization and enhancement of the normalized iris template by illumination compensation and contrast enhancement techniques. To compare these normalized templates, textural features are extracted. Data obtained from the images should prepare appropriate Criterion for identification and differentiation between the patterns and also must be compressed as much as possible to minimize the required memory for data storage and to increase the speed of authentication process [23].

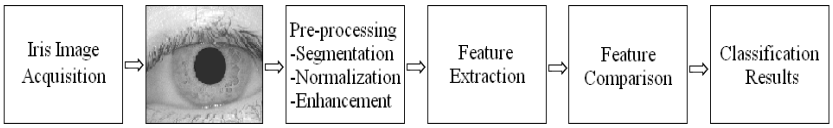

Figure 1. The Architecture of the Iris Recognition System

Although various techniques have been designed to locate the iris region but the most important algorithms that are used in most studies have been proposed by Daugman and Wildes.

In Daugman's method, pupillary and limbic boundaries of the eye have been approximated as non-concentric circles. Thus, a boundary could be described with three parameters: radius r, and the coordinates of the center of the circle (x_c,y_c). He proposed

an integro-differential operator for detecting the iris boundary by searching the parameter space.

$$\max(r, x_c, y_c) \left| G_\sigma(r) * \frac{\partial}{\partial r} \oint_{r,x_c,y_c} \frac{\mathbf{I}(x,y)}{2\pi r} ds \right| \quad (1)$$

where $G_\sigma(r)$ is a smoothing function such as a Gaussian of scale σ and $\mathbf{I}(x,y)$ is the original image of the eye. The complete operator behaves as a circular edge detector that searches over the candidate domain iteratively with respect to increasing radius r for maximum contour integral derivative [3, 6-10].

Wildes employed an automatic segmentation algorithm based on the circular Hough transform to locate the iris region. In his method, firstly an edge map is generated by calculating the first derivatives of intensity values in an eye image and then thresholding the result. From the edge map, votes are cast in Hough space for the parameters of circles passing through each edge point [11-13]. These parameters are the centre coordinates (x_c,y_c), and the radius r, which are able to define any circle according to equation (2).

$$x_c^2 + y_c^2 - r^2 = 0 \quad (2)$$

After the iris region is isolated from the eye image, this region is transformed to a normalized rectangular template using Daugman's rubber sheet model. This method remaps each point within the iris region to a pair of polar coordinates (r,θ) in order to produce a normalized representation with constant dimensions. The remapping of the iris region is modeled as below.

$$\mathbf{I}(x(r,\theta), y(r,\theta)) \rightarrow \mathbf{I}(r,\theta) \quad (3)$$

where $\theta \in ([3\pi/4, 5\pi/4] \cup [7\pi/4, 9\pi/4])$ is the sampling angle and $r \in [0,1]$ is the normalized distance between each sampling point and the pupillary boundary according to the iris width in each angle [11].

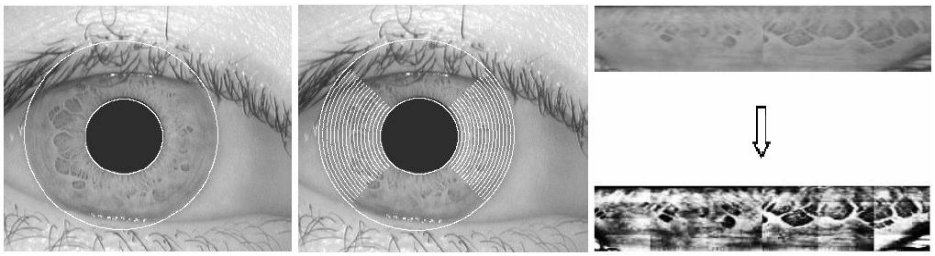

(a) (b) (c)

Figure 2. Image Pre-processing: (a) Localization of the Iris Region, (b) Unwrapping and Normalization, (c) Enhancement of the Normalized Iris Template

It is necessary to improve the contrast of the normalized template for iris feature extraction since it has low contrast as shown in Figure 2(c) (Top). After compensating illumination differences in the image, histogram stretching and equalization techniques

are used to obtain an iris image with enhanced contrast as shown in Figure 2(c) (Bottom).

Although a recognition system can use the unwrapped iris directly to compare two irises, most systems first use a feature extraction routine to encode the iris's textural content. Encoding algorithms generally perform a multi-resolution analysis of the iris by applying wavelet filters and examining the ensuing response. In a commonly used encoding mechanism, 2D Gabor wavelets are first used to extract the local phasor information of the iris texture; the mechanism then encodes each phasor response using two bits of information, resulting in a binary iris code. Gabor wavelets are complex Gaussian damped sinusoids. The following equation shows the feature extraction process using polar form of 2D Gabor wavelet.

$$h\{\mathrm{Re},\mathrm{Im}\} = Sgn\{\mathrm{Re},\mathrm{Im}\}\iint e^{-j\omega(\theta-\theta')} \cdot e^{-(r-r')^2/\alpha^2} \cdot e^{-(\theta-\theta')^2/\beta^2} \mathbf{I}(r,\theta) r dr d\theta \tag{4}$$

where α , β and ω are parameters related to the scale and frequency of the wavelet; the angle θ′ and the radial distance r′ provide the polar location of the filter [3, 6-10].

Another approach for extracting features and encoding the normalized iris image is the cumulative sum based gray change analysis method. This algorithm generates iris codes by analyzing the changes of gray values of iris patterns. Upward slope of cumulative sums means that iris pattern may change from darkness to brightness; downward slope of cumulative sums means the opposite change of upward slope [24].

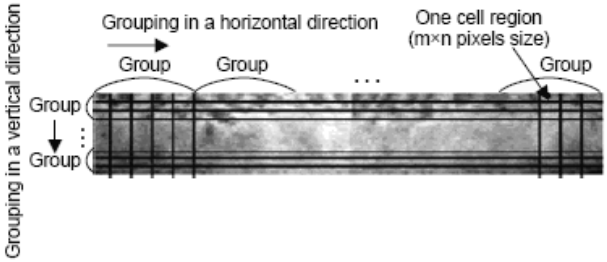

Figure 3. Division of Normalized Iris Image into Basic Cell Regions and Grouping of Cell Regions [25]

Overall feature extraction process is as follows.

Step 1. Divide normalized iris image into basic cell regions for calculating cumulative sums. One cell region has m × n pixels size. An average gray value is used as a representative value of a basic cell region to calculate the cumulative sum.

Step 2. Basic cell regions are grouped horizontally and vertically as shown in Figure 3.

Step 3. Calculate cumulative sums over the each group.

Step 4. Generate iris feature codes.

Cumulative sums are calculated as follows. Suppose that X_1, X_2, ... , X_5 are five representative values of each cell region within the first group located on the left top corner of Figure 3.

- Calculate the average:

$$\overline{X} = (X_1 + X_2 + ... + X_5)/5 \quad (5)$$

- Calculate cumulative sum from 0: $S_0 = 0$.
- Calculate the other cumulative sums by adding the difference between the current value and the average to the previous sum:

$$S_i = S_{i-1} + (X_i - \overline{X}) \quad \text{for} \quad i = 1,2,...,5 \quad (6)$$

The cumulative sums begin from 0 and end at 0. After calculations, iris codes are generated for each cell by analyzing sums [25]. The iris code is set to 1 for cells that located on the upward slope (left side of the MAX value or right side of the MIN value) and is set to 0 for others [24].

During enrollment, the system saves encoded features into a database. During authentication, after performing pre-process steps like enrollment stage and extracting features, the system compares the presented iris against all database codes to verify a claimed identity or identify an individual. There are different algorithms to compare the input code with the codes saved in the database of the identification system; among them, calculating the Hamming distance is the most common method used for measuring the similarity between the binary codes. A lower Hamming distance indicates higher similarity.

$$HD = \frac{1}{N}(\sum_{i=1}^{N} A_i \oplus B_i) \quad (7)$$

where A_i and B_i denote the enrolled iris code and the new input code respectively; N is total number of cells and $\oplus$ is the XOR operator [11].

One of the other techniques that used for this purpose is the neural network; in this regard, networks with parallel combination of several Rosenblatt's perceptrons [4] and networks with multi-layer perceptron (MLP) architecture [5] are used in pervious studies.

While the noise resistance of the MLP networks is weak and they are usually unable to classify the noisy patterns correctly, many factors such as ambient lighting reflections, change in the angle of the user's head during image acquisition process or occlusions like eyelashes or eyelids or even the use of contact lenses are cause noise in the input images.

In this paper, a combination of cumulative sum based gray change analysis method for encoding the iris patterns and fuzzy ARTMAP neural network for comparing the iris codes is used to deal with the input noise. Although the algorithm of the feature extraction method is consisted of simple calculations, but the obtained codes have good resistance against the input noise; fast learning ability and high noise resistance, also make fuzzy ARTMAP neural networks one of the best options for pattern classification purposes.

3. Fuzzy ARTMAP Neural Network

Fuzzy ARTMAP, achieves a synthesis of fuzzy logic and Adaptive Resonance Theory (ART) neural networks by exploiting a close formal similarity between the computations of fuzzy subsethood and ART category choice, resonance and learning. Because this neural network architecture has a small number of parameters and requires no problem-specific system crafting or choice of initial weight values, it is also easy to use. Although off-line training of fuzzy ARTMAP by applying the shuffled training set exemplars in a number of epochs increases the classification accuracy of this network, where an epoch is defined as one cycle of training on an entire set of input exemplars, one way in which this kind of network differs from many previous fuzzy pattern recognition algorithms is incremental or on-line learning; it means that fuzzy ARTMAP is also able to learn each input as it is received on-line, rather than performing an off-line optimization of a criterion function [26].

Each ARTMAP system includes a pair of adaptive resonance theory modules (ART_a and ART_b) that create stable recognition categories in response to arbitrary sequences of input patterns; these modules are linked by an inner ART module F^{ab} (also called map field) which is to determine whether the correct mapping has been established from inputs to outputs. Each ART system includes a field, F_0, of nodes that represent a current input vector; a field, F_1, that receives both bottom-up input from F_0 and top-down input from a field, F_2, that represents the active category (Figure 4). Associated with each F_2 category node j (j = 1,...,N) is a vector $\boldsymbol{w}_j \equiv$ (w_{j1},...,w_{jM}) of adaptive weights. Initially $w_{j1}(0) = \cdots = w_{jM}(0) = 1$; then each category is said to be uncommitted. After a category is selected for coding it becomes committed [27].

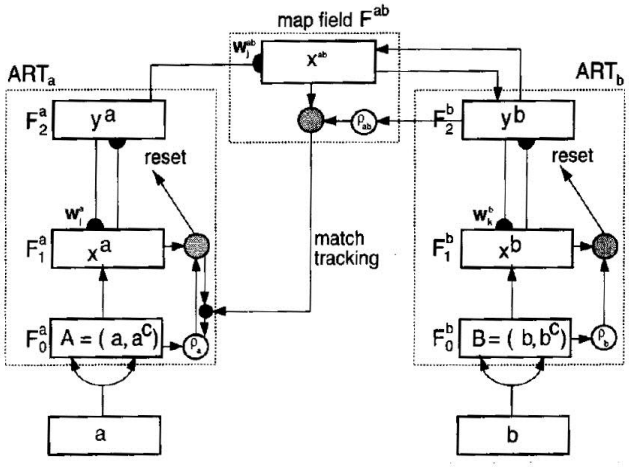

Figure 4. Fuzzy ARTMAP Architecture [26]

Adaptive resonance theory modules create recognition categories based on the training patterns presented to the system. ART_b is used for training ART_a and after completing the training phase, this module is discarded and the output is determined by applying the input patterns to ART_a. During supervised learning, ART_a receives a stream $\{\mathbf{a}^{(p)}\}$ of input patterns and ART_b also receives a stream $\{\mathbf{b}^{(p)}\}$ of patterns, where $\mathbf{b}^{(p)}$ is the correct prediction given $\mathbf{a}^{(p)}$. These modules are linked by an internal controller that ensures autonomous system operation in real-time; the controller is designed to create

the minimal number of ART_a recognition categories, needed to meet accuracy criteria [27].

The steps of fuzzy ARTMAP algorithm are summarized as follows.

1. Input data:

The input pattern of ART_a is represented by the vector **a** = [a_1,...,a_{Ma}] and the input pattern of ART_b is represented by the vector **b** = [b_1,...,b_{Mb}] [26].

2. Parameters:

There are three fundamental parameters corresponding to the performance and learning of fuzzy ART network [26].

- Choice parameter, ($\alpha > 0$): which acts on the category selection.
- Learning rate parameter, ($\beta \in [0,1]$): that controls the velocity of network adaptation.
- Vigilance parameter, ($\rho \in [0,1]$): that controls the network resonance. The vigilance parameter is responsible for the number of formed categories.

3. Algorithm structure:

- Complement coding is a normalization rule that preserves amplitude information and represents both on-response and off-response to an input vector. The complement coded input **I** to the field F_1 is the 2M-dimensional vector [26].

$$\mathbf{I} = (\mathbf{a}, \mathbf{a}^c) \equiv (a_1,...,a_M, a_1^c,...,a_M^c) \tag{8}$$

- For each input **I** and F_2 node j, the choice function T_j is defined by

$$T_j(\mathbf{I}) = \frac{\left|\mathbf{I} \wedge \mathbf{w}_j\right|}{\alpha + \left|\mathbf{w}_j\right|} \tag{9}$$

where the fuzzy AND operator $\wedge$ is defined by

$$(\mathbf{p} \wedge \mathbf{q})_i \equiv \min(p_i, q_i) \tag{10}$$

and where the norm | . | is defined by

$$|\mathbf{p}| \equiv \sum_{i=1}^{M} |p_i| \tag{11}$$

The system is said to make a category choice when at most one F_2 node can become active at a given time. The category choice is indexed by j, where T_j = max { T_j : j = 1...N }. If more than one T_j is maximal, the category j with the smallest index is chosen. In particular, nodes become committed in order j = 1, 2, 3, ... When the jth category is chosen, y_j = 1; and y_i = 0 for $i \neq j$ [26].

- Resonance occurs if the match function of the chosen category *j*, meets the vigilance criterion:

$$\frac{\left|\mathbf{I} \wedge \mathbf{w}_j\right|}{\left|\mathbf{I}\right|} \geq \rho \tag{12}$$

Otherwise, the value of the choice function T_j is set to zero for the duration of the input presentation to prevent the persistent selection of the same category during search. A new index *j* is then chosen and the search process continues until the chosen category satisfies (12) [26].

4. Learning:

Once search ends, the weight vector $\boldsymbol{w}_j$ is updated. The adaptation of the ART_a and ART_b module weights is given by

$$\mathbf{w}_j^{(new)} = \beta(\mathbf{I} \wedge \mathbf{w}_j^{(old)}) + (1-\beta)\mathbf{w}_j^{(old)} \tag{13}$$

Fast learning corresponds to setting $\beta = 1$ [26].

5. MAP field activation:

The map field F^{ab} is activated whenever one of the ART_a or ART_b categories is active. If node *j* of F_2^a is chosen, then its weights $\boldsymbol{w}_j^{ab}$ activate F^{ab}. If node *k* in F_2^b is active, then the node *k* in F^{ab} is activated by 1-to-1 pathways between F_2^b and F^{ab}. If both ART_a and ART_b are active, then F^{ab} becomes active only if ART_a predicts the same category as ART_b via the weights $\boldsymbol{w}_j^{ab}$. The F^{ab} output vector $\boldsymbol{x}^{ab}$ obeys

$$\boldsymbol{x}^{ab} = \begin{cases} \mathbf{y}^b \wedge \mathbf{w}_j^{ab} & \text{if the } j\text{th } F_2^a \text{ node is active and } F_2^b \text{ is active} \\ \mathbf{w}_j^{ab} & \text{if the } j\text{th } F_2^a \text{ node is active and } F_2^b \text{ is inactive} \\ \mathbf{y}^b & \text{if } F_2^a \text{ is inactive and } F_2^b \text{ is active} \\ \mathbf{0} & \text{if } F_2^a \text{ is inactive and } F_2^b \text{ is inactive [26].} \end{cases} \tag{14}$$

4. Experimental Results

All the experiments were carried out on a system with Intel Pentium M 1.8 GHz processor and 512 MB of RAM using MATLAB 7.8.0 software and CASIA V1.0 [28] eye image database. This database consists of 756 eye images from 108 people; for each person, 3 pictures were captured during the first session and remaining 4 were captured in the second session.

To evaluate the accuracy and the noise resistance of the cumulative sum feature extraction technique, two 90 degree cones were selected from both sides of the iris circular region detected by Wildes' method; after remapping the selected pixels into polar coordinates and performing normalization process using Daugman's rubber sheet model, a 60 × 300 pixels template was produced from each eye image. After enhancing the quality of these templates by performing illumination compensation and contrast enhancement procedures, their textural characteristics were extracted by using both

2D Gabor wavelets and cumulative sum based gray change analysis methods and two 1800-bit binary codes were produced from each template; in order to calculate the similarity of iris codes, Hamming distance method was used.

To simulate the real-world application, systems were trained to identify 60 individuals using all 180 images of subjects captured during the first session; then the false rejection rate (FRR) was calculated using 240 images of these authorized users captured during the second session. To calculate the false acceptance rate (FAR), the remaining 336 images that belong to unauthorized individuals were used.

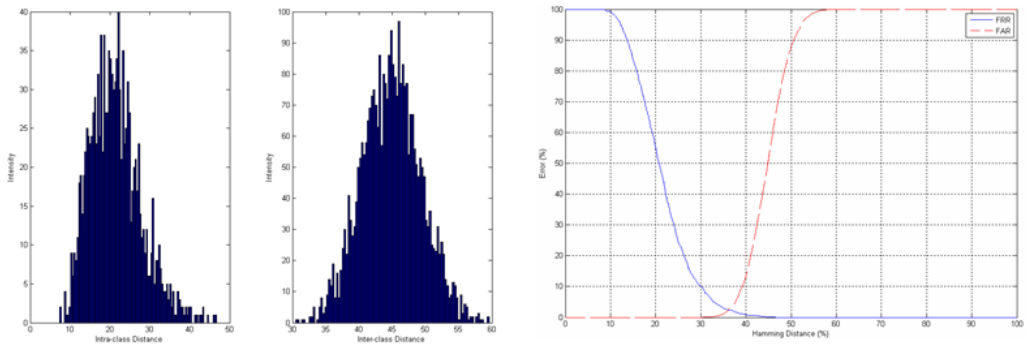

(a) (b) (c)

Figure 5. Accuracy of the identification system which uses Gabor wavelets Feature Extraction Method: (a) Intra-class Hamming Distance Distribution, (b) Inter-class Hamming Distance Distribution, (c) FAR/FRR Curves According to the Hamming Distance

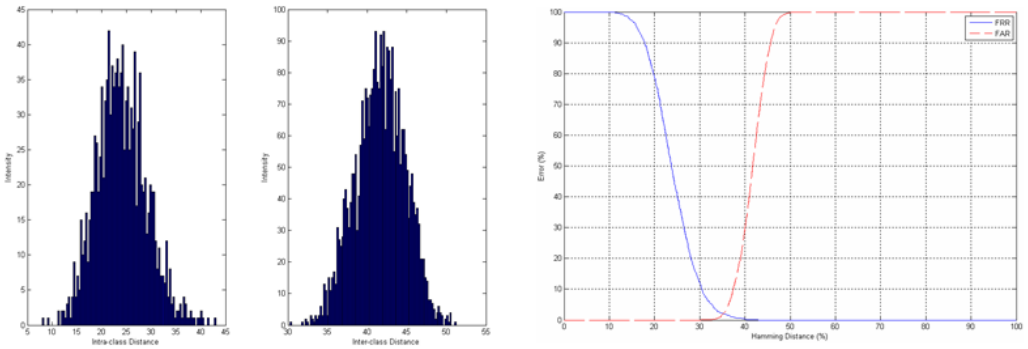

(a) (b) (c)

Figure 6. Accuracy of the Identification System which uses Cumulative Sum Feature Extraction Method: (a) Intra-class Hamming Distance Distribution, (b) Inter-class Hamming Distance Distribution, (c) FAR/FRR Curves According to the Hamming Distance

The system which uses Gabor wavelets for feature encoding propose is able to correctly identify authorized individuals from impostors with 2.38% equal error rate (EER) when the threshold is 36.08; the other system which takes advantage of the cumulative sum method, achieves less than 2.06% EER when the threshold is 35.23. The accuracy of both identification systems are shown in Figures 5 and 6.

Although iris codes produced by both methods almost have the same accuracy but minimum Hamming distances achieve by 1 pair of shifts in cumulative sum codes, while Gabor wavelet codes need 3 pairs; therefore, we can conclude that the cumulative sum has a better resistance against the change of user's head angle than the other method. Performance of the feature extraction techniques according to the number of shifts is shown in Table 1 and Figure 7.

Table 1. Accuracy According to the Number of Shifts in Hamming Distance Calculation

Number of Shifts	Feature Extraction Method			
	Gabor Wavelet		*Cumulative SUM*	
	EER (%)	Threshold	EER (%)	Threshold
0	*3.58*	*38.34*	*2.173*	*35.34*
1	*2.78*	*37.16*	*2.06*	*35.23*
2	*2.62*	*36.34*	*2.06*	*35.23*
3	*2.38*	*36.08*		
4	*2.38*	*36.08*		

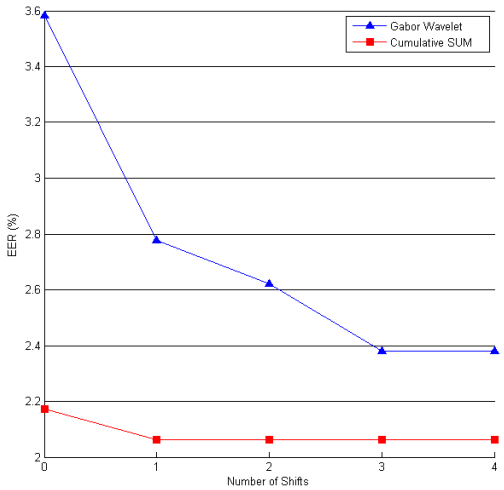

Figure 7. Error of the Feature Extraction Methods According to the Number of Shifts

To assess the classification performance of fuzzy ARTMAP network, 1800-bit cumulative sum codes were used. During the training phase and for both ART modules, the learning rate parameter β is considered equal to 1 in order to achieve the fastest learning performance and the choice parameter α is considered equal to 0.001 in order to speed up the selection of the winner category. During the test phase, the choice parameter of ART_a is remained the same and the vigilance parameter of this module is such increased that the FAR is reduced to zero; when this goal is achieved, the FRR is also reduced by increasing the number of the training patterns used for each authorized user. Accordingly, in the first step a single training image is used for introducing each authorized person to system; by increasing the vigilance parameter ρ_a to 0.72, FAR is dropped to zero and 32.5% FRR is obtained. The FRR is then reduced to 14.17% by

using a pair of training images for each user and by using all three images captured in the first session, the FRR is also reduced to zero and an accurate and noise resistant identification system is successfully designed. The accuracy of this identification system according to the vigilance parameter of ART_a is shown in Figure 8.

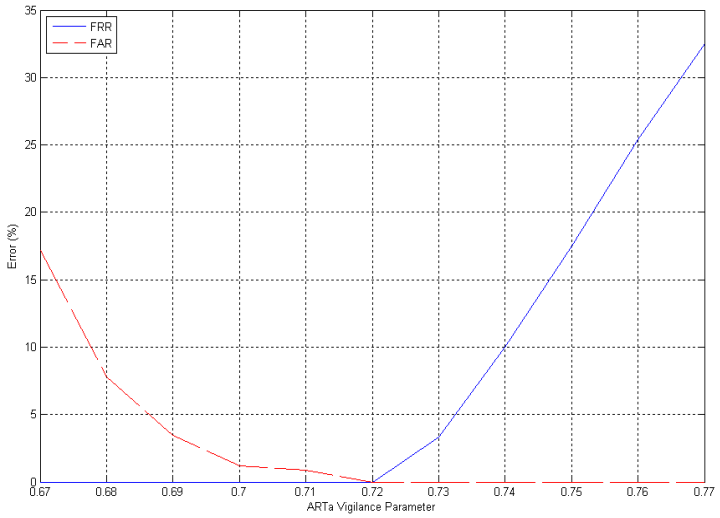

Figure 8. FAR/FRR Curves According to the Vigilance Parameter of ART_a

The vigilance parameter determines the minimum consistency between the input and the reference code, to be detected as similar patterns. The ARTMAP network training results according to use of different vigilance parameters is shown in Table 2. By increasing the vigilance parameter during the training phase, the number of categories and thus the network classification accuracy increases. Thereupon, ρ_a and ρ_b and also ρ_{ab} are considered equal to 1; so, during the training phase separate classification categories are created in ART modules for each new training pattern. In this mode, the network only refuses to register repetitive patterns.

Table 2. Performance of the System According to the Vigilance Parameter

Training		Testing		
ART_a Vigilance Parameter	No. ART_a Categories	ART_a Vigilance Parameter	FAR (%)	FRR (%)
0.7	*113*	*0.72*	*0*	*86.67*
0.8	*154*	*0.72*	*0*	*27.5*
0.9	*179*	*0.72*	*0*	*0*
1	*180*	*0.72*	*0*	*0*

The proposed system is able to identify all 60 enrolled users with 100% accuracy and without accepting even one unauthorized person. The average time required for authentication of each input code is almost 10 times faster than the Hamming distance method and takes less than 0.0008 seconds.

Table 3 demonstrates the accuracy rate of the proposed system in compare with the other conventional approaches.

Table 3. Accuracy Rate of Iris Recognition Systems on CASIA Database

Methodology	Accuracy rate (%)
Boles [15]	*92.61*
Li Ma [17]	*94.33*
Wang [21]	*97.25*
Daugman [6]	*99.37*
Proposed	*100*

Due to the results shown in table 3, it is clear that the proposed system has the best identification performance on CASIA database among all the existing methods.

5. Conclusion

The input images are almost certainly noisy; thus, the accuracy of the identification system rises by the use of noise resistant feature extraction and classification algorithms such as cumulative sum based gray change analysis method and fuzzy ARTMAP neural network. Despite its low computational complexity, this feature encoding technique has a very good noise resistance; fuzzy ARTMAP networks are also able to classify input patterns correctly even if more than 30% of them have been affected by noise; so, even by using 1800-bit iris codes, which are shorter than those that used by Daugman, the proposed system still achieves the best possible accuracy.

Another advantage of this classification method compared with perceptron based networks is incremental or on-line learning; therefore, the database of the system can be quickly edited without performing time-consuming off-line learning process.

The results of simulations on CASIA iris database illustrate that an accurate and noise resistant personal identification system has been successfully designed by using a combination of the mentioned methods; however, in future studies it is necessary to do experiments on more eye image databases for iris recognition system to be more reliable.

References

[1] A. Jain, R. Bolle, S. Pankanti, "Biometrics: Personal Identification in a Networked Society", Kluwer Academic Publishers, **(1999)**.
[2] F. Adler, "Physiology of the Eye: Clinical Application", Fourth edition: The C.V. Mosby Company, London **(1965)**.
[3] John G. Daugman, "Biometric Personal Identification System Based on Iris Analysis", US Patent, no. 5291560, **(1994)**.
[4] M. Gopikrishnan and T. Santhanam, "Neural Network Based Accurate Biometric Recognition and Identification of Human Iris Patterns", Journal of Computer Science, vol. 6, no. 10, **(2010)**, pp. 1170-1173.
[5] R. H. Abiyev and K. Altunkaya, "Personal Iris Recognition Using Neural Network", International Journal of Security and its Applications, vol. 2, no. 2, **(2008)** April, pp. 41-50.
[6] J. G. Daugman, "High Confidence Visual Recognition of Persons by a Test of Statistical Independence", IEEE Transactions on Pattern Analysis and Machine Intelligence, vol. 15, no. 11, **(1993)**, pp. 1148-1161.
[7] J. G. Daugman and C. Downing, "Recognizing iris texture by phase demodulation", IEEE Colloquium on Image Processing for Biometric Measurement, vol. 2, **(1994)**, pp. 1-8.
[8] J. G. Daugman, "Statistical Richness of Visual Phase Information: Update on Recognizing Persons by Iris Patterns", International Journal of Computer Vision, vol. 45, no. 1, **(2001)**, pp. 25-38.
[9] J. G. Daugman, "Demodulation by Complex-Valued Wavelets for Stochastic Pattern Recognition", International Journal of Wavelets, Multi resolution and Information Processing, vol. 1, no. 1, **(2003)**, pp. 1-17.
[10] J. G. Daugman, "How iris recognition works", IEEE Transactions on Circuits and Systems for Video Technology, vol. 14, **(2004)** January, pp. 21-30.

[11] L. Masek, "Recognition of Human Iris Patterns for Biometric Identification", Report for Bachelor of Engineering degree, Presented to the School of Computer Science and Software Engineering, The University of Western Australia, **(2003)**.
[12] R. Wildes, J. Asmuth, G. Green, S. Hsu, R. Kolczynski, J. Matey and S. McBride, "A Machine-Vision System for Iris Recognition", Machine Vision and Applications, vol. 9, **(1996)**, pp. 1-8.
[13] R. Wildes, "Iris Recognition: An emerging Biometric Technology", IEEE Proceedings, vol. 46, no. 4, **(1998)**, pp. 1185-1188.
[14] L. Ma, Y. H. Wang and T. N. Tan, "Iris recognition based on multichannel Gabor filtering", Proceedings of the Fifth Asian Conference on Computer Vision, **(2002)**; Australia, pp. 279-283.
[15] W. Boles and B. Boashash, "A Human Identification Technique Using Images of the Iris and Wavelet Transform", IEEE Transactions on Signal Processing, vol. 46, no. 4, **(1998)**, pp. 1185-1188.
[16] C. Sanchez-Avila and R. Sanchez-Reillo, "Iris-Based Biometric Recognition Using Dyadic Wavelet Transform", IEEE Aerospace and Electronic Systems Magazine, **(2002)**, pp. 3-6.
[17] L. Ma, T. Tan, Y. Wang and D. Zhang, "Personal Identification Based on Iris Texture Analysis", IEEE Transaction on Pattern Analysis and Machine Intelligence, vol. 25, no. 12, **(2003)**.
[18] S. Lim, K. Lee, O. Byeon and T. Kim, "Efficient Iris Recognition through Improvement of Feature Vector and Classifier," ETRI Journal, vol. 23, no. 2, **(2001)**, pp. 61-70.
[19] C. Tisse, L. Martin, L. Torres and M. Robert, "Person Identification Technique Using Human Iris Recognition", Proceedings of Vision Interface, **(2002)**, pp. 294-299.
[20] Y. -P. Huang, S. -W. Luo and E. -Y. Chen, "An Efficient Iris Recognition System," Proceedings of the First International Conference on Machine Learning and Cybernetics, **(2003)** November; Beijing, China.
[21] Y. Wang and J. -Q. Han, "Iris Recognition Using Independent Component Analysis", Proceedings of the Fourth International Conference on Machine Learning and Cybernetics, **(2005)**; Guangzhou, China.
[22] V. Dorairaj, N. Schmid and G. Fahmy, "Performance Evaluation of Iris Based Recognition System Implementing PCA and ICA Techniques", Proceedings of SPIE 2005 Symposium, **(2005)**; Orlando, USA.
[23] M. J. Brown, "Singular Value Decomposition & 2D Principal Component Analysis of Iris Biometrics for Automatic Human Identification", Master of Science Thesis, Presented to Russ College of Engineering & Technology, Ohio University, **(2006)** June.
[24] J. G. Ko, Y. H. Gil, J. H. Yoo and I. Chung, "Method of Iris Recognition using Cumulative-Sum-Based Change Point Analysis and Apparatus using the same", U.S. Patent Application Publication, Pub. no.: US 0014438 A1, **(2007)** January.
[25] J. G. Ko, Y. H. Gil, J. H. Yoo and I. Chung, "A Novel and Efficient Feature Extraction Method for Iris Recognition", ETRI Journal, vol. 29, no. 3, **(2007)** June, pp. 399- 401.
[26] G. A. Carpenter, S. Grossberg, N. Markuzon, J. H. Reynolds and D. B. Rosen, "Fuzzy ARTMAP: A Neural Network Architecture for Incremental Supervised Learning of Analog Multidimensional Maps", IEEE Transactions on Neural Networks, vol. 3, no. 5, **(1992)** September, pp. 698-713.
[27] G. A. Carpenter, S. Grossberg and J. H. Reynolds, "Fuzzy ARTMAP, Slow Learning, and Probability Estimation", Boston University Center for Adaptive Systems and Department of Cognitive and Neural Systems, **(1993)** January.
[28] Center for Biometrics and Security Research, Institute of Automation, Chinese Academy of Sciences; Iris Image Database (CASIA V1.0), **(2011)** June, http://www.cbsr.ia.ac.cn/IrisDatabase.htm.

Authors

Arash Taherian received the B.Sc. degree in electric power engineering from Islamic Azad University South Tehran Branch in 2005. He is currently a master's student in control engineering at the Faculty of Graduate Studies, IAU South Tehran Branch. His research interests include Neural Networks, Fuzzy Systems and Pattern Recognition.

Mahdi Aliyari Sh. received the B.Sc. degree in electronics engineering, the M.Eng. degree and Ph.D. degree in control engineering from K. N. Toosi University of Technology, in 2001, 2003 and 2008, respectively. He is currently an Assistant Professor with the Department of Mechatronics Engineering, K. N. Toosi University of Technology, Tehran. He is the author of more than 120 papers in international journals and conference proceedings. His research interests include Fault Tolerant, detection and diagnosis, Intelligent control of Mechatronics systems and Multi objective optimization.